

# Generalized Bipolariton Model. Propagation of a Ultrashort Laser Pulse Through a Thin Semiconductor Film in the Conditions of Two-Photon Generation of Biexcitons

Igor BELOUSSOV

*Institute of Applied Physics, Academy of Sciences of Moldova*  
igor.beloussov@phys.asm.md

**Abstract** — A generalized bipolariton model is proposed. Bipolaritons is formed from virtual excitons of four kinds. There exists both attractive and repulsive interaction between these excitons, though only excitons of a specific type can interact with light. A substantial difference between conventional [1] and our models is shown for the case of nonlinear transmission/reflection of ultrashort laser pulses by a thin semiconductor film under two-photon generation of biexcitons.

**Index Terms** — biexciton, bipolariton, thin semiconductor film, ultrashort laser pulse.

## I. INTRODUCTION

Ivanov, Keldysh, and Haug pointed out several problems of phenomenological giant oscillator strength model in [1] and proposed a self-consistent theory of two-photon excitations based on bipolariton conception. According to [1] the following scheme seems to be adequate: an exciton is considered as a true boson, however, biexciton is treated as a compound particle, i.e., the bound states of two excitons due to the interaction potential  $W(\mathbf{r}-\mathbf{r}')$ . Obviously such interaction has to be attractive. But as it is known from the quantum liquid theory, at low temperatures the system of Bose-particles with attractive interaction is unstable against spontaneous contraction. In order to avoid this difficulty two equivalent kinds of excitons  $\sigma = \pm 1$  with the same parameters may be introduced. The only distinction is that excitons of different kinds attract each other ( $W_{+,-1} = W_{-,-1} < 0$ ), whereas particles of the same kind have a repulsive interaction ( $W_{-,-1} = W_{+,+1} > 0$ ). Such an approach simultaneously leads to the existence of bound complexes of two excitons of different kinds and the stability of the many-particle system as a whole. The proposed model may be considered as corresponding to the singlet excitons with mutually opposite directions of an electron (and also hole) spin.

The conventional *bipolariton model* developed in [1] deals with the term

$$H_{x-x} = \frac{1}{2V} \sum_{\sigma, \sigma_1 = \pm 1} \sum_{\mathbf{k}_1, \mathbf{k}_2, \mathbf{q}} W_{\sigma, \sigma_1}(q) a_{\mathbf{k}_1, \sigma}^\dagger a_{\mathbf{k}_2, \sigma_1}^\dagger a_{\mathbf{k}_2 + \mathbf{q}, \sigma_1} a_{\mathbf{k}_1 - \mathbf{q}, \sigma} \quad (1)$$

of the full Hamiltonian that describes the exciton-exciton interactions. This model was further experimentally tested by measuring the two-photon transition width, nonlinear susceptibility  $\chi^{(3)}$ , two-photon absorption coefficient [50], and the angular dependence of the biexciton luminescence under resonant two-photon excitation,

yielding a better agreement compared with the giant oscillator strength model.

The main difference of the model presented by Hamiltonian (1), from the real one is the absence of triplet excitons that do not dipole-interact with photons but play an important role in the formation of biexcitons. A more realistic model includes four kinds of excitons with different values of spin projection of the electron and of the hole. The interaction of exciton of any kind with excitons of all other kinds is repulsive on the average. The pairs of excitons with antiparallel spins of electrons as well as of holes interact attractively and biexcitons can be formed.

Let us consider a model of the crystal with band structure containing the conduction band spin degenerate only and the double degenerate valence band where the hole states are characterized by the total momentum  $J$  and its projection  $J_z$ . Assume that the energy of dissociation of the biexciton considerably exceeds the energy of ortho-para splitting. This condition is realized, for example, in bulk CuCl, CuBr and CdS crystals, in which biexcitons have been detected experimentally. The interaction Hamiltonian of the four kinds of excitons in this case can be written as

$$H_{x-x} = \frac{1}{2V} \sum_{\mathbf{k}_1, \mathbf{k}_2, \mathbf{q}} \left\{ \frac{1}{4} [3v_{ss}(\mathbf{k}_1, \mathbf{k}_2; \mathbf{k}_1 + \mathbf{q}, \mathbf{k}_2 - \mathbf{q}) + v_{aa}(\mathbf{k}_1, \mathbf{k}_2; \mathbf{k}_1 + \mathbf{q}, \mathbf{k}_2 - \mathbf{q})] \sum_{j=1}^4 a_{\mathbf{k}_1, j}^\dagger a_{\mathbf{k}_2, j}^\dagger a_{\mathbf{k}_2 - \mathbf{q}, j} a_{\mathbf{k}_1 + \mathbf{q}, j} + v_{ss}(\mathbf{k}_1, \mathbf{k}_2; \mathbf{k}_1 + \mathbf{q}, \mathbf{k}_2 - \mathbf{q}) \sum_{\substack{j=1 \\ (i \neq j)}}^4 a_{\mathbf{k}_1, i}^\dagger a_{\mathbf{k}_2, j}^\dagger a_{\mathbf{k}_2 - \mathbf{q}, j} a_{\mathbf{k}_1 + \mathbf{q}, i} \right.$$

$$\begin{aligned}
 & + \frac{1}{4} [v_{aa}(\mathbf{k}_1, \mathbf{k}_2; \mathbf{k}_1 + \mathbf{q}, \mathbf{k}_2 - \mathbf{q}) \\
 & - v_{ss}(\mathbf{k}_1, \mathbf{k}_2; \mathbf{k}_1 + \mathbf{q}, \mathbf{k}_2 - \mathbf{q})] \sum_{\substack{i,j=1 \\ (i \neq j)}}^3 a_{\mathbf{k}_1,i}^\dagger a_{\mathbf{k}_2,i}^\dagger a_{\mathbf{k}_2-\mathbf{q},j} a_{\mathbf{k}_1+\mathbf{q},j} \\
 & + \frac{1}{4} [v_{ss}(\mathbf{k}_1, \mathbf{k}_2; \mathbf{k}_1 + \mathbf{q}, \mathbf{k}_2 - \mathbf{q}) \\
 & - v_{aa}(\mathbf{k}_1, \mathbf{k}_2; \mathbf{k}_1 + \mathbf{q}, \mathbf{k}_2 - \mathbf{q})] \\
 & \times \sum_{i=1}^3 [a_{\mathbf{k}_1,i}^\dagger a_{\mathbf{k}_2,i}^\dagger a_{\mathbf{k}_2-\mathbf{q},4} a_{\mathbf{k}_1+\mathbf{q},4} + a_{\mathbf{k}_1,4}^\dagger a_{\mathbf{k}_2,4}^\dagger a_{\mathbf{k}_2-\mathbf{q},i} a_{\mathbf{k}_1+\mathbf{q},i}] \}.
 \end{aligned} \quad (2)$$

For bulk CuCl the index  $i=1,2,3$  of the creation,  $a_{\mathbf{k},i}^\dagger$ , and annihilation,  $a_{\mathbf{k},i}$ , operators of excitons corresponds to the rows of the irreducible representation  $\Gamma_5(x)$ ,  $\Gamma_5(y)$ , and  $\Gamma_5(z)$ , while  $i=4$  corresponds to  $\Gamma_2$ . If the electromagnetic field is polarized in the plane  $(x, y)$  of the semiconductor film, then only excitons with  $i=1,2$  dipole-interact with it, but excitons with  $i=3,4$  do not.

Using (2) we can obtain the set of equations for the positive-frequency parts of the electric field strength and macroscopic amplitudes of excitons and biexcitons is simplified using some approximations that correspond to the physical assumptions. As a result a closed set of ordinary differential equations is found. The results of the numerical calculations of the set of equations are presented and discussed in the next section.

### I. NUMERICAL RESULTS

The dynamics of the pulses transmitted and reflected by the film can be investigated by a numerical integration of the set of dynamical equations. Further we assume that the incident on the semiconductor film laser pulse is Gaussian with duration  $t_p$ :

$$f(t) = \exp \left[ -2 \left( \frac{t-t_0}{t_p} \right)^2 \right]. \quad (3)$$

Its maximum intensity is given by  $S = |E_{in}(t_0)|^2 / 2\pi$ .

Fig. 1 shows that the behavior of the transmission function

$$T(\bar{t}) = |E_t(\bar{t})|^2 / |E_{in}(\bar{t}_0)|^2$$

for the incident pulse with duration  $t_p = 1 ps$  and thin film with thickness  $L = 10^{-5} cm$  substantially depends on the pulse intensity  $S$ . Here  $E_{in}(\bar{t}) = f(\bar{t}) E_{in}(\bar{t}_0)$ , and  $E_t(\bar{t})$  is the envelope of the transmitted electromagnetic field. In the conditions of exact resonance ( $\Delta^m = 0$ ) and low excitation levels ( $S \leq 100 MW/cm^2$ ) the transmission function exhibits a peak, whose front weakly distinguishes from the incident pulse. We will name this peak the main part of transmitted pulse. The amplitude and duration of the main part of transmitted pulse is lower than the amplitude and duration of the incident pulse, respectively. The maximum of the transmitted pulse precedes the maximum of the incident pulse (superlight

transmission). This leading increases when  $S$  increases; the amplitude and duration of the main part of transmitted pulse decrease. A trailing tail follows the main part of transmitted pulse in the form of a sequence of subpulses with low and quickly decreasing amplitudes. For small  $S$  ( $\leq 40 MW/cm^2$ ) these subpulses are located on the distant trailing tail of the incident pulse. When  $S$  increases and the main part of transmitted pulse compresses, the subsequent train of subpulses shifts to the centre of the incident pulse.

We use the function

$$R(\bar{t}) = |E_r(\bar{t})|^2 / |E_{in}(\bar{t}_0)|^2$$

to describe the radiation reflected by the film. Here  $E_r(\bar{t})$  is the envelope of the reflected electromagnetic field. For  $S = 40 MW/cm^2$ , at the time interval, which corresponds to the trailing tail of the transmitted pulse and follows the rear of the incident pulse, the irregular reflection peaks are present. They are absent for  $S \leq 20 MW/cm^2$ . When  $S$  further increases, a part of them becomes suppressed; but the other part becomes narrower, more intensive and shifts to the centre of the incident pulse. Their maximal amplitude can exceed the amplitude of incident pulse.

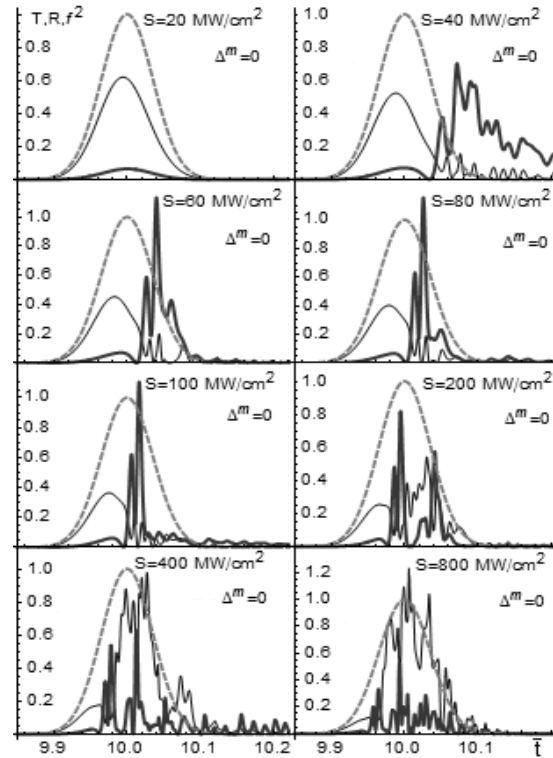


**Fig. 1.** Transmission function  $T(\bar{t}) = |E_t(\bar{t})|^2 / |E_{in}(\bar{t}_0)|^2$  (blue), reflection function  $R(\bar{t}) = |E_r(\bar{t})|^2 / |E_{in}(\bar{t}_0)|^2$  (red) and function  $f^2(\bar{t}) = |E_{in}(\bar{t})|^2 / |E_{in}(\bar{t}_0)|^2$  (green) for various values of the incident pulse intensity  $S = |E_{in}(\bar{t}_0)|^2 / 2\pi$ . Pulse duration  $t_p = 1 ps$  and film thickness  $L = 10^{-5} cm$ .

Consequently, for very low excitation levels ( $S \leq 20 \text{ MW/cm}^2$ ) the incident pulse practically does not change when it passes through the film. For medium excitation levels ( $S \leq 100 \text{ MW/cm}^2$ ) the incident pulse undergoes a substantial transformation. The main part of transmitted pulse is formed accompanied by ripples of small subpulses. The narrow and intensive pulses of reflected radiation arise.

When the intensity of the incident pulse continues to increase ( $S > 100 \text{ MW/cm}^2$ ) the dependences  $T(\bar{t})$  and  $R(\bar{t})$  become more complicated. As can be seen in Fig. 1, the main part of transmitted pulse is eventually suppressed and series of irregular transmission and reflection pulses arise. Their location is limited by the duration of the incident pulse. Usually the minima (or inflection points) of the transmission function  $T(\bar{t})$  correspond to the maxima of the reflection function  $R(\bar{t})$ . Two first high and narrow reflection peaks shift to the range of the front of the incident pulse and their amplitude decreases simultaneously (superlight reflection); additional sharp peaks arise.

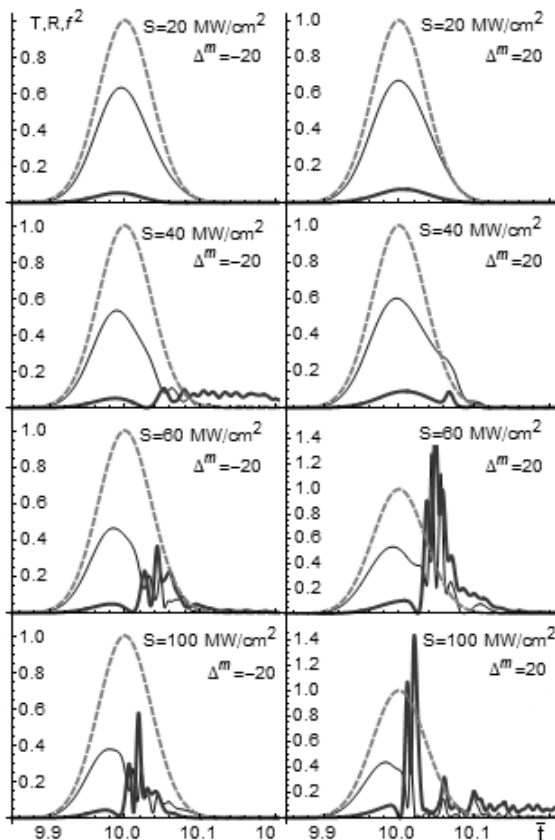


**Fig. 2.** Transmission function  $T(\bar{t})$  (blue), reflection function  $R(\bar{t})$  (red) and function  $f^2(\bar{t})$  (green) for various values of the incident pulse intensity  $s$ . Pulse duration  $t_p = 1 \text{ ps}$ , film thickness  $L = 10^{-5} \text{ cm}$ , resonance detuning  $\Delta^m = -20$  (left) and  $\Delta^m = 20$  (right).

The structure of the transmitted and reflected pulses becomes more complicated when the intensity of the incident pulse increases. This can be caused by a complex nonlinear interference of the forward and backward waves of the electromagnetic radiation propagating through the film and also by the interference of the waves of the excitonic and biexcitonic polarizations of the medium. The constructive (destructive) interference of waves near the front end of the films results in the appearance (vanishing) of the sharp and narrow reflection peaks. The constructive (destructive) interference of waves near the rear end of the film leads to the appearance (vanishing) of the transmission peaks.

The increasing of the number of the transmission and reflection peaks with the increasing of the intensity of the incident radiation is caused by the dependence of the interaction constants at nonlinear terms in the set of our equations from  $S$ .

Consider the peculiarities of transmission (reflection) of the Gaussian pulse that appear when the resonance detuning  $\Delta^m$  is finite. Fig. 2 shows the results only for  $\Delta^m = \pm 20$  and low excitation levels. In both the cases ( $\Delta^m = -20$  and  $\Delta^m = +20$ ), the profiles of the transmitted and reflected pulses in the range of the rear of the incident pulse change when its intensity increases. These changes are larger for  $\Delta^m > 0$ . Similar to the case of  $\Delta^m = 0$ , when the excitation level increases, these changes start to fill the whole range of the incident pulse.

Fig. 3 shows the evolution of the transmitted and reflected pulses for the fixed incident pulse intensity  $S = 70 \text{ MW/cm}^2$  and various values of the resonance detuning  $\Delta^m$ . When the detuning increases for  $\Delta^m < 0$ , the rear of the incident pulse distorts, and reflection peaks eventually arise on it. In the vicinity  $\Delta^m = 0$  they enhance considerably; simultaneously, the transmission contains only the main part of transmitted pulse and several low subpulses. For  $\Delta^m > 20$  the transmitted pulse regains its Gaussian shape; its maximum is delayed with respect to the maximum of the incident pulse. For  $-60 < \Delta^m < 0$  the maximum of the transmitted radiation precedes the maximum of the incident pulse. For very large values  $|\Delta^m|$  the transmitted and reflected pulses exhibit practically the same shape as the incident pulse.

When the duration of the incident pulse reduces, the subpulses of transmission and reflection in its trailing tail enhance. This effect appears since a strong inversion of the medium is created in a short time interval, which then slowly spreads in the process of its induced radiative decay. A nonstationary polarization of the medium induced by a very short pulse can exist during the time interval that exceeds the duration of the pulse.

On the contrary, when the pulse duration increases, all the radiation processes and the formation of the transmission and reflection subpulses primarily occur during the time of action of the pulse. The number of the transmission and reflection peaks increases considerably. It is interesting that for negative resonance detunings the formation of very high and narrow reflection pulses is possible, though the transmission is practically absent.

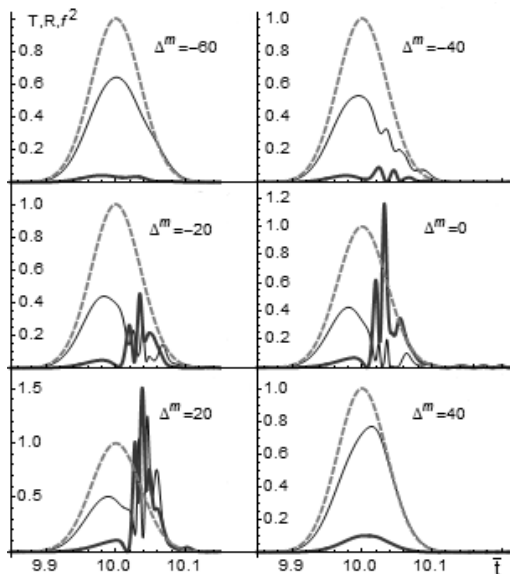


**Fig. 3.** Transmission function  $T(\bar{\tau})$  (blue), reflection function  $R(\bar{\tau})$  (red) and function  $f^2(\bar{\tau})$  (green) for various values of the resonance detuning  $\Delta^m$ . Pulse intensity  $S = 70 \text{ MW/cm}^2$ , pulse duration  $t_p = 1 \text{ ps}$  and film thickness  $L = 10^{-5} \text{ cm}$ .

Even more interesting picture appears, when both the pulse duration and the film thickness increase. In this case, depending on the detuning  $\Delta^m$ , the reflection function  $R(\bar{\tau})$  can exhibit a sequence of series of very narrow peaks or a single giant peak in the rear of the incident pulse (Fig. 4). Increasing the intensity of the incident pulse one can shift this peak to the front of the incident pulse (superlight reflection).

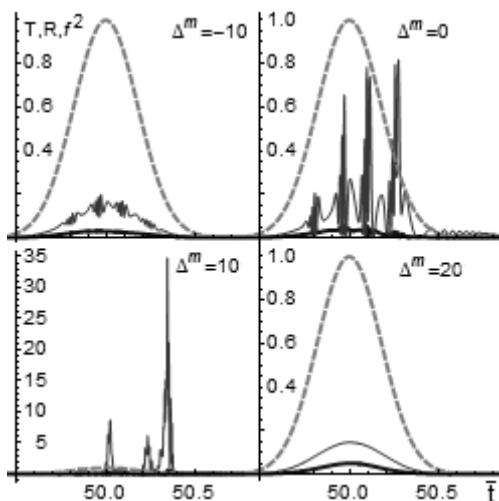


**Fig. 4.** Transmission function  $T(\bar{\tau})$  (blue), reflection function  $R(\bar{\tau})$  (red) and function  $f^2(\bar{\tau})$  (green) for various values of the resonance detuning  $\Delta^m$ . The incident pulse intensity  $S = 90 \text{ MW/cm}^2$ , pulse duration  $t_p = 5 \text{ ps}$  and film thickness  $L = 10^{-4} \text{ cm}$ .

In the framework of the model proposed in [1] the dependences of transmission  $T(\bar{\tau})$  and reflection  $R(\bar{\tau})$  are described by the curves that substantially differ from

those shown in Fig. 1 (see Fig. 5). When the intensity of the incident pulse increases, the transmission function  $T$  undergoes more significant changes than the reflection function  $R$ . At first (for  $S > 40 \text{ MW/cm}^2$ ), the transmission in the central range of the incident pulse becomes suppressed; simultaneously two peaks in its trailing tail enhance. One of them increases and shifts to the front of the incident pulse. As a result, a narrow transmission peak surrounded by two satellites arises in the centre of the incident pulse. When the excitation level continues to increase ( $S > 400 \text{ MW/cm}^2$ ), the dependence  $T(\bar{\tau})$  becomes oscillating with a sharp transmission peak at the rear of the incident pulse. The main difference of these results from those shown in Fig. 1 is that the high and narrow reflection peaks are absent in the simple model of two kinds of excitons [1].

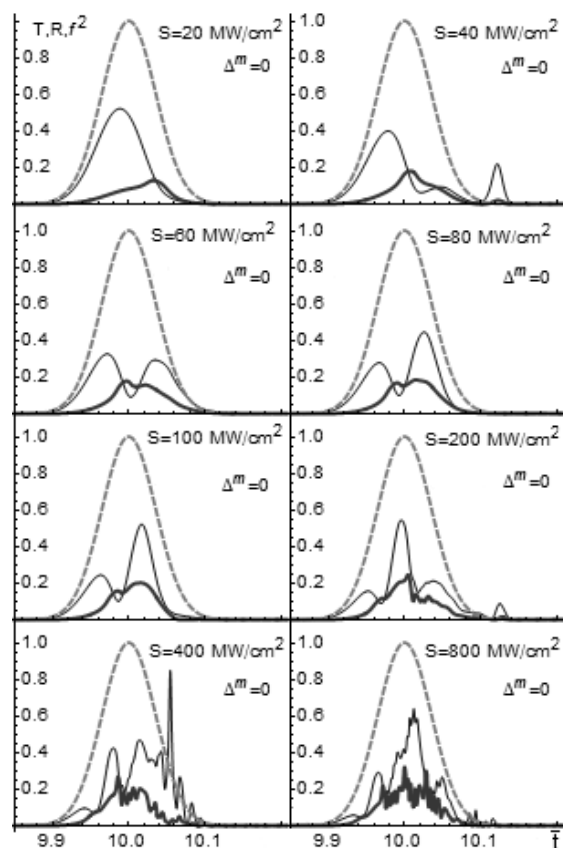


**Fig. 5.** Transmission function  $T(\bar{\tau})$  (blue), reflection function  $R(\bar{\tau})$  (red), and function  $f^2(\bar{\tau})$  (green) for various values of the incident pulse intensity  $s$  obtained in the simple model of two kinds of excitons.[1]. Pulse duration  $t_p = 1 \text{ ps}$  and film thickness  $L = 10^{-5} \text{ cm}$ .

The numerical solution of these equations for the parameters  $t_p = 1 \text{ ps}$  and  $L = 10^{-5} \text{ cm}$  show that the transmission function is almost of the Gaussian form and its maximal value increases with the increasing of the excitation level. The reflection function also has the Gaussian form with weak oscillations in its contour. The frequency of the oscillations increases when the excitation level increases; the maximal value of the reflection function is small and practically does not change. The

plots of both the functions are limited by the contour of the incident pulse. This result gives evidence that only one shift of the energy of excitons dependent on their density cannot lead to substantial peculiarities of the dynamics of the transmitted and reflected pulses shown in Figs. 1-4. On the other hand, as follows from Fig. 5, these peculiarities are absent when the noted shift is not taken into account. Therefore, the complicated behavior of the functions  $T(\bar{t})$  and  $R(\bar{t})$  is caused by a combined action of three nonlinearities existing in the system and by the relationships between their coefficients. These relationships depend on the amplitude of the incident pulse.

Note, that in the giant oscillator strength model the shifts of energy levels of exciton and biexciton dependent on the exciton density are also absent. Therefore, it is not surprising that the results obtained in the framework of this model are described by simple dependences substantially different from those presented in Figs. 1-4.

### CONCLUSION

Figs. 1-4 show that the functions of transmission and reflection of ultrashort pulses of laser radiation in the conditions of two-photon excitation of biexcitons exhibit a complicated shape and several bright peculiarities caused by combined nonlinear interactions present in the system.

At very low excitation levels the incident pulse passes through the film practically unchanged; at medium excitation levels it significantly changes. The most interesting for potential application is the fact that narrow peaks of transmission (for  $\Delta^m > 0$ ) and reflection appear at specific conditions; the height of these peaks can considerably exceed the amplitude of the incident pulse.

The results are very sensitive to the choice of such the parameters as the film thickness  $L$ , resonance detuning  $\Delta^m$ , intensity of the incident pulse  $S$ , its duration  $t_p$ , and also substantially depend on the relationships between the interaction constants. Their calculation is a separate complicated problem. However, the values of interaction constants can be found from other simpler experiments. For example, the constant  $\nu_1$  can be determined from the experiments related to the generation of excitons by resonance photons ( $\Delta^x \approx 0$ ). The constant  $\nu_2$  can be found from the experiment at low excitation levels, when the role of nonlinear terms associated with the shift of the exciton and biexciton energy levels is insignificant.

### REFERENCES

- [1] A.L. Ivanov, H. Haug, and L.V. Keldysh, Phys. Rep., vol. 296, pp. 238, 1998.